Proceedings of the ASME 2010 International Mechanical Engineering Congress & Exposition
IMECE 2010
November 12-18, Vancouver, British Columbia, Canada

IMECE2010-39008

INVESTIGATION OF THE EFFECTIVENESS AND EFFICIENCY OF THE EXACT CLOSURE: COMPARISON WITH INDUSTRIAL CLOSURES AND SPHERICAL HARMONIC SOLUTIONS

Babatunde O. Agboola
Baylor University
Dept. of Mechanical Engineering
Waco, Texas 76798, U.S.A
Babatunde_Agboola@Baylor.edu

David A. Jack
Baylor University
Department of Mechanical Engineering
Waco, TX 76798, U.S.A.
David_Jack@Baylor.edu

Stephen Montgomery-Smith
University of Missouri – Columbia
Department of Mathematics
Columbia, MO 65211, U.S.A.
stephen@missouri.edu

Douglas E. Smith
University of Missouri – Columbia
Department of Mechanical and Aerospace Engineering
Columbia, MO 65211, U.S.A.
smithdoug@missouri.edu

ABSTRACT

For stiffness predictions of short fiber reinforced polymer composites, it is essential to understand the orientation during processing. This is often performed through the equation of change of the fiber orientation tensor to simulate the fiber orientation during processing. Unfortunately this approach, while computationally efficient, requires the next higher ordered orientation tensor, thus requiring the use of a closure approximation. Many efforts have been made to develop closures to approximate the fourth-order orientation tensor in terms of the second order orientation tensor. Recently, Montgomery-Smith et al (2010) developed a pair of exact closures, one for systems with dilute suspensions and a second for dense suspensions, where the later works well for a variety of diffusion models. In this paper we compare the fiber orientation results of the Fast Exact Closure (FEC) for dense suspensions to that of the Spherical Harmonic solution, which although considered to be numerically exact does not readily lend itself to implementations in current industrial processing CFD codes. This paper focuses on a series of comparisons of material stiffness predictions between the FEC, current fitted closure models, and the spherical harmonics solution for a thin plate subjected to pure shear. Results for the select flows considered show the similarities between the current class of orthotropic fitted closures and that of the FEC. Although the results are similar between the fitted closures and the FEC, it is important to recognize that the Fast Exact Closure is formed without a fitting process. Consequently, the results are anticipated, in general, to be more robust in implementation.

INTRODUCTION

Industrial design of short-fiber reinforced polymer composites, which are frequently employed in injection molded composites, requires understanding the relationship between the processing, the structure, and the resulting structural and thermal properties of the resulting part. Due to their specific properties and ease of manufacturing, short fiber polymer composites have experienced considerable industrial usage. During manufacturing, flow creates patterns of deferential fiber orientation within the parts. This leads to considerable point-to-point variation and anisotropy in the mechanical properties of the material. Several properties of interest for the final processed part include the stiffness, warpage, shrinkage, thermal expansion, strength of the cured composite, and the thermal and electrical conductivities. During processing, it is understood that the fiber orientation also alters the effective shear stress as the thermal and electrical conductivity of the liquid state during product processing. Of interest in the present study is the prediction of the stiffness of the cured composite, which is known to be highly dependent on the orientation of the fibers. The final processed product's structural response is highly dependent on understanding the final fiber orientation's microstructure.

The Folgar-Tucker diffusion model [1] is frequently used for modeling the short-fiber orientation of dense suspensions within a thermoplastic [1-2]. Unfortunately, direct computations of the Folgar-Tucker model of orientation require considerable computational resources, and thus is not directly applicable for engineering design use [3]. Orientation tensors (also called the moments of the fiber orientation distribution function) are an alternative to represent the state of fiber orientation. This approach is widely used as it offers a concise representation of the orientation states thus allowing easy and efficient computations [4-5]. Unfortunately, the application of

the orientation tensor equation of motion requires the next higher even-ordered tensor [4,6]. This requirement may be alleviated through the use of tensor closures/approximations, where most authors choose to close the fourth-order orientation tensor using information from the second-order orientation tensor.

The orientation tensor approach was first popularized by Advani and Tucker [4,7] when they introduced the Hybrid closure. Their closure has been extensively used to model the spatially varying orientation distribution function within a macroscopic part [6]. Although the fourth-order hybrid closure is computationally efficient with accuracies beyond that of the outdated linear [8] and quadratic [9] closures, the hybrid closure tends to over predict the actual fiber alignment [4]. The relative inaccuracy of the hybrid closure was improved by Cintra and Tucker [10] in their orthotropic closure. The orthotropic closure of Cintra and Tucker has been further modified by authors like Han and Im [11], VerWeyst *et al.* [12] and Chung and Kwon [13]. Verleye and Dupret [14] developed the natural closure which was modified by Petty *et al.* [15] and further improved by Chung and Kwon [16].

Jack *et al*. [5] introduced the use of artificial neural networks as a new class of closures. They computed the fourth-order orientation tensor from the corresponding second-order tensors using artificial neural networks (ANN). The ANN was reported to be as accurate as the orthotropic fitted closure of Cintra and Tucker [10] at a computational expense that approaches that of the less accurate hybrid closure of Advani and Tucker [4]. It was shown that although the NNET performed well over many flows of concentrated suspensions, the NNET failed in flows that couple shearing with biaxial elongation and had accuracies worse than that of the hybrid closure. In addition, the NNET was observed to experience oscillatory behavior for semi-concentrated suspension flows, which is defined as

$$1 \leq nL^3 \leq \frac{L}{d} \tag{1}$$

where n is the number of fibers per unit volume in the suspension, L is the fiber length and d is the fiber diameter.

Najam and Jack [17] employed the ANN approach to create a coordinate frame invariant Neural Network-Based orthotropic closure (NNORT). As will be shown in this paper, the NNORT has accuracies representing the orientation and stiffness equal to or greater than current industrially employed closures, with only nominal computational increases beyond that of the orthotropic closures over all flow conditions studied.

Recently, Montgomery *et al.* [18-20] have developed a pair of exact closures, one for systems with dilute suspensions [18][18] and a second called the Fast Exact Closure (FEC) for dense suspensions [19-20] where the later works quite well for a variety of diffusion models and fiber concentrations.

An investigation into the effectiveness and efficiency of these new closures is the motivation for the present paper. Fiber orientation results from the classical closures, the Neural Network closures and novel FEC will be presented and compared with the exact solutions of fiber orientation obtained from the Spherical Harmonic approach [21]. The spherical harmonic approach expands the orientation distribution function, $\psi(\theta,\phi)$, using the complex spherical harmonics Y_l^m [22] to any desired order as [21]

$$\psi(\theta,\phi) = \sum_{l=0}^{\infty} \sum_{m=-l}^{l} \hat{\psi}_l^m Y_l^m \tag{2}$$

where $\hat{\psi}_l^m$ are the complex spherical harmonic coefficients that contain information pertaining to the orientation. The equation of motion for $\psi(\theta,\phi)$, $\frac{\mathrm{D}\psi}{\mathrm{Dt}}$, is expanded using Equation (2) and transient solutions of $\frac{\mathrm{D}\psi}{\mathrm{Dt}}$ using the Spherical Harmonic expansion approach will be considered as the basis for our analysis for solutions from closure approaches. This new algorithm is exceptionally efficient as compared to solutions using the control volume method, and exhibits accuracies only limited by machine precision. These solutions are considered exact in the present study, and using the techniques in [21] we have solutions used in the present study that are accurate to the 8th significant digit throughout the entire flow evolution. These solutions will be used to confirm the accuracy of the selected closure. In the following paper we will compare the orientation results from several of the aforementioned closures with those obtained from the Spherical Harmonic solutions, and present results showing the impact the inaccuracies in the fiber orientation have on the subsequent material properties.

SHORT-FIBER REINFORCED POLYMER COMPOSITES FLOW MODELING

Industrially used process simulation models for short fiber based composites are based on the equation of motion for fiber orientation distribution $\psi(\theta,\phi,t)$ given by Folgar and Tucker [1]. This model was developed to combine the motion of non-interacting rigid ellipsoids within a Newtonian fluid through Jeffery's equation [23] and the motion of interacting particles through the use of the empirically determined interaction coefficient C_I to simplify the complex fiber collision processes.

The computation of the orientation distribution function is quite verbose, and the compact and computationally efficient method of orientation tensors proposed by Advani and Tucker [4] is often employed. A code that evaluates $\psi(\theta,\phi,t)$ directly using the control volume approach for simple flows with an interaction coefficient of $\mathrm{C_I} \approx 10^{-4}$ can take several weeks to months to reach the steady state orientation [6,17,24], whereas solutions using the Spherical Harmonic approach will require several minutes [21]. Solutions of the orientation tensor equation of motion

for the same flows can be solved in a matter of seconds. Due to this exceptional computational efficiency, the orientation tensor method is more favored industrially [10]. Equation (3) gives the definition of the orientation tensor. This is based on the dyadic products of the unit vector $\mathbf{p}(\theta,\phi)$ and integrating the product of these tensors with the orientation distribution function over all possible directions. This is done over a unit sphere S^2 and written as

$$a_{ij} = \oint_{S^2} p_i p_j \psi(\theta,\phi) dS$$
$$a_{ijkl} = \oint_{S^2} p_i p_j p_k p_l \psi(\theta,\phi) dS \quad (3)$$
$$a_{ij\dots} = \oint_{S^2} p_i p_j \cdots \psi(\theta,\phi) dS$$

where p_i is the i^{th} component of the unit vector $\mathbf{p}(\theta,\phi)$. Orientation tensors are fully symmetric i.e. $a_{ij} = a_{ji}$ and $a_{ijkl} = a_{jikl} = a_{klij} = \cdots$. Based on the normalization condition of the distribution function $\int_{S^2} \psi(\theta,\phi) dS = 1$, it can be shown that the lower order orientation tensor can be completely described by the higher order orientation tensors through the commutatively property of the integrand. Thus Equation (3) yields the following relationships

$$a_{ii} = 1, \qquad a_{ij} = a_{ijpp}, \qquad a_{ijkl} = a_{ijklqq} \quad (4)$$

where repeated indices imply summation, i.e. $a_{ii} = a_{11} + a_{22} + a_{22}$. The equation of motion for the computation of second order orientation tensor given in Advani and Tucker [4] is expressed as

$$\frac{Da_{ij}}{Dt} = -\frac{1}{2}\left(\omega_{ik}a_{kj} - a_{ik}\omega_{kj}\right) + \frac{1}{2}\lambda\left(\gamma_{ik}a_{kj} + a_{ik}\gamma_{kj} - 2\gamma_{kl}a_{ijkl}\right) + 2C_I\dot{\gamma}(\delta_{ij} - 3a_{ij}) \quad (5)$$

where $\dot{\gamma}$ is the scalar magnitude of the rate of deformation tensor γ_{ij}, $\omega_{ij} = v_{j,i} - v_{i,j}$ is the vorticity tensor where v_i is the i^{th} component of the velocity vector, and λ is a function of the fiber aspect ratio r_e which can be written as $\lambda = ({r_e}^2 - 1)/({r_e}^2 + 1)$. As can be seen in Equation (5), the equation of change of the second order orientation tensor a_{ij} requires the fourth order orientation tensor a_{ijkl}, thus bringing about the need for a closure approximation.

CLOSURE APPROXIMATIONS

Fourth order closure approximations can be generalized as

$$a_{klmn} \approx f_{klmn}(a_{ij}) \quad (6)$$

It is noted, that an objective closure must be independent of the choice of coordinate frame [10]. a_{ijkl} symmetric fourth order tensor can be represented and displayed as a 6×6 matrix of components using contracted notation [10]. Each component a_{ijkl} can be written as A_{mn}, where m corresponds to the ij components and n corresponds to the kl components. When ij or kl = 11, m or n will be, respectively, replaced by 1. Similarly, when ij or kl = 22 the m or n component will be replaced by 2, if ij or kl = 33 m or n will be replaced by 3. When ij or kl = 23 or 32 m or n are replaced by 4. When ij or kl = 31 or 13 m or n are replaced by 5, and lastly when ij or kl = 12 or 21 m or n are replaced by 6. Based on the symmetric nature of the orientation tensor (see Equation (4)), the general fourth order orientation tensor has at most 15 independent components (which is further reduced to 14 due to the fact that $a_{iijj} = a_{ii} = 1$).

Hybrid Closure (HYB)

The hybrid closure [4] is a very popular choice of a closure because of its algebraic simplicity and numerical robustness, despite some well known drawbacks [7]. It is formed from a linear combination of the quadratic closure of Doi [8] and the linear closure of Hand [9]. The linear closure was developed by using all linear products of the second order orientation tensor a_{ij} and the identity tensor δ_{ij}, whereas the quadratic closure is formed by simply taking the product of lower-order tensors as $\hat{a}_{ijkl} = a_{ij}a_{kl}$ [8]. The hybrid closure was a significant improvement over the previously existing closures, and has been used over a wide range of fiber orientation distributions and concentrations [4]. The fourth order hybrid closure is given as

$$a_{ijkl} = (1-f)\hat{a}_{ijkl} + \bar{a}_{ijkl} \quad (7)$$

where $\hat{a}_{ijkl}$ is the linear closure, $\hat{a}_{ijkl}$ is the quadratic closure, and f is a generalization from Herman's orientation factor; that is equal to zero for randomly oriented fibers and unity for perfectly aligned fibers [4] Investigations of the Folgar and Tucker equation with the hybrid closure are of industrial interest, as this closure approximation is frequently used in commercial codes for 3D injection molding simulations [2].

Orthotropic Closure (ORT)

The orthotropic closure approximations significantly improved on the accuracy of the hybrid closure, but often at the cost of an increase in the computational efforts. [10-13]. Among the orthotropic closure approximations, those that go through a fitting process, as compared to those that are exact for select orientation states, provide the most accurate results when compared to experimentally measured fourth-order orientation tensors [25]**.** The orthotropic closures rely on either the eigenvalues or the invariants of the second-order orientation tensor. The eignevalues of the second order orientation tensor a_{ij} expressed as $a_{(i)}, i \in \{1,2,3\}$, subject to the constraint $1 \geq a_{(1)} \geq a_{(2)} \geq a_{(3)}$. Based on the normalization condition it

can be seen that $a_{(1)} + a_{(2)} + a_{(3)} = 1$, thus the second-order orientation tensor has two independent eigenvalues [10]. One final constraint for the orthotropic closures is the assumption that all objective fourth-order closure formulas are necessarily orthotropic, with the principal axes of the second- and the fourth-order orientation tensor being the same [10]. Thus, in the principal frame, the objective fourth-order orientation tensor, in contracted notation, can be expressed as

$$\overline{\mathbf{A}} = \begin{bmatrix} \overline{A}_{11} & \overline{A}_{12} & \overline{A}_{13} & 0 & 0 & 0 \\ \overline{A}_{12} & \overline{A}_{22} & \overline{A}_{23} & 0 & 0 & 0 \\ \overline{A}_{13} & \overline{A}_{23} & \overline{A}_{33} & 0 & 0 & 0 \\ 0 & 0 & 0 & \overline{A}_{44} & 0 & 0 \\ 0 & 0 & 0 & 0 & \overline{A}_{55} & 0 \\ 0 & 0 & 0 & 0 & 0 & \overline{A}_{66} \end{bmatrix} \quad (8)$$

Notice that when written in the principal frame, many of the components of the fourth-order orientation tensor are zero. The orthotropic closures assume the remaining nonzero components of $\tilde{A}_{mn}$ are reasonably expressed as a function of the eigenvalues, $a_{(1)}$ and $a_{(2)}$. The orientation tensor $\bar{A}_{mn}$ can be further reduced based on the contraction from the fourth- to the second-order orientation tensor along with the symmetries from Equation (3) to 9 components. The fourth-order tensor can be further reduced recognizing that [10]

$$A_{44} = a_{2323} = a_{2233} = A_{23} = A_{32} \quad (9)$$

$$A_{55} = a_{1313} = a_{1133} = A_{13} = A_{31} \quad (10)$$

$$A_{66} = a_{1212} = a_{1122} = A_{12} = A_{21} \quad (11)$$

Using the contracted notation along with Equations (9)-(11), the fourth-order tensor can be expressed in the principal frame as

$$\bar{A}_{11} + \bar{A}_{66} + \bar{A}_{55} = a_{(1)} \quad (12)$$

$$\bar{A}_{66} + \bar{A}_{22} + \bar{A}_{44} = a_{(2)} \quad (13)$$

$$\bar{A}_{55} + \bar{A}_{44} + \bar{A}_{33} = a_{(3)} = 1 - a_{(1)} - a_{(2)} \quad (14)$$

This introduces three additional constraints, thereby reducing the unknown components of $\tilde{A}$ to three, $\bar{A}_{11}$, $\bar{A}_{22}$ and $\bar{A}_{33}$ [10]. For the orthotropic closures these are typically assumed to be functions of eigenvalues $a_{(1)}$ and $a_{(2)}$. For the ORT closure used by VerWeyst *et al.* [12] the expression to generate the fourth-order tensor from the second-order tensor is

$$\bar{A}_{mm}^{closure} = C_m^1 + C_m^2 a_{(1)} + C_m^3 [a_{(1)}]^2 + C_m^4 a_{(2)} + C_m^5 [a_{(2)}]^2 + C_m^6 a_{(1)} a_{(2)} \quad (15)$$

Neural Network Based Closure (NNET)

The Neural Network Based Closure (NNET) is based on an Artificial Neutral Network (ANN) which mimics the biological signal processing scheme. ANNs assume that information processing takes place at discrete neurons or elements, and signals between links are carried by the neurons with a predetermined offset or amplification, which are given by, respectively, the weight and bias contained in each link [5]. This closure was motivated by a quest for a closure approximation which stands between the computationally efficient hybrid closure and the accurate orthotropic closures [5]. The composition of a neural network includes an input layer, one or more hidden layers, where information processing takes place by modifying the inputs using controlled training parameters, and an output layer. The operation of a single neuron neural network is expressed mathematically as

$$y = f(wx + b) \quad (16)$$

where x is the scalar connected to the first neuron with amplification and offset given by, respectively, the weight w and bias b, and f is the activation function which operates on the resulting neuron to produce the output y.

The Neural Network Orthotropic Closure (NNORT) closure [17] improves on the NNET in that it is truly objective and coordinate frame invariant. It combines the architecture of the ANN while maintaining the principles of the orthotropic closures. The NNORT is based on a network where the output is computed as

$$\bar{A}_4 = f_2(w_2 . f_1(w_1 . \bar{A}_2 + b_1) + b_2) \quad (17)$$

where $\bar{A}_4$ is a 3×1 array consisting of the three unknown components of $\bar{A}_{mn}$ from Equations (12)-(14) and $\bar{A}_2$ is a 2×1 array consisting of the $a_{(1)}$ and $a_{(2)}$. w_2 is the $n \times 3$ array of weights connecting the hidden layer to the output layer (n being the number of neurons in the hidden layers), b_1 is the $n \times 1$ array of biases associated with the hidden layer, b_2 is the 3×1 array of biases associated with the output layer, and f_1 and f_2 are the hyperbolic tangent and the pure linear transfer functions, respectively [17]. w_1 is an $n \times 2$ array of weights connecting the input layer to the hidden layer. Equation (17) is employed along with Equations (9)-(14) to compute the fourth order orientation tensor in the principal frame and then rotated into to the laboratory reference frame with the eigenvectors of a_{ij}.

Fast Exact Closure (FEC)

The Fast Exact Closure (FEC) [19-20] is not a closure approximation in the traditional sense as it does not rely upon an approximation based on select orientation states of the fourth-moment. The complete description of the FEC is given in the related IMECE'2010 paper [20], and is only briefly discussed in the present paper. The FEC is a fast method for solving Jeffery's equation for a variety of diffusion (fiber collision) models, and does not rely on any curve fitting techniques nor does it rely on an elliptic integral computation. The approach relies on solving a series of related ordinary differential equations and bypasses the fitting process. This approach is called exact in the sense that in the absence of diffusion will exactly solve the Jeffery's equation. It also carries with it the ability to solve the tensor

equations of motion for many of the alternative diffusion models. The FEC for the Jeffery's equation with isotropic diffusion is generated by simultaneously solving the ODEs for the symmetric second-order tensors **a** and **b**, where **a** is the second-order orientation tensor

$$\frac{D\mathbf{a}}{Dt} = \frac{1}{2}\mathbb{C}\colon[\mathbf{b}\cdot(\boldsymbol{\Omega}+\lambda\boldsymbol{\Gamma})\cdot\mathbf{b}] + D_r(2\mathbf{I}-6\mathbf{a}) \tag{18}$$

$$\frac{D\mathbf{b}}{Dt} = -\frac{1}{2}(\mathbf{b}\cdot(\boldsymbol{\Omega}+\lambda\boldsymbol{\Gamma}) + (-\boldsymbol{\Omega}+\lambda\boldsymbol{\Gamma})\cdot\mathbf{b}) - D_r\mathbb{D}\colon(2\mathbf{I}-6\mathbf{a}) \tag{19}$$

The form of the equations of motion for several popular anisotropic diffusion forms can be seen in the papers presented by Montgomery-Smith *et al* [19-20]. In Equations (18) and (19) $\mathbb{C}$ is a rank 4 symmetric tensor computed with respect to the basis of the orthonormal eigenvectors of **b** and can be obtained directly from the eigenvalues of **a** and **b** (see [19-20]). $\mathbb{D}$ is the rank-four tensor that is the inverse of the fourth-order tensor $\mathbb{C}$ and is defined with respect to the basis of eigenvalues of **b**. The tensors **Ω**, **Γ**, and **I** are the vorticity, rate-of-deformation, and identity tensors, respectively. Montgomery-Smith *et al.* [19-20] demonstrate that it can be quite numerically efficient to perform the intermediate calculations involved in computing $\frac{D\mathbf{a}}{Dt}$ and $\frac{D\mathbf{b}}{Dt}$ completely in the coordinate system of eigenvalues of **b**, and rotate the resulting second-order orientation tensors **a** and **b** as opposed to performing the rotations on the fourth-order orientation tensor. As can be observed in Equations (18) and (19), there is no need for the classical closure of Equation (6) as there is no fourth-order orientation tensor appearing in either of the equations of motion. An exhaustive study of the exact closures can be seen in the papers written by Montgomery-Smith *et al.* [18-20].

STIFFNESS PREDICTION

The elastic properties of a short fiber reinforced composite require an understanding of the underlying unidirectional stiffness matrix along with the fiber orientation distribution function [4,26]. The stiffness tensor of the processed short-fiber reinforced composite is based upon an orientationally biased summation of the properties of the underlying unidirectional microstructure of a single fiber within the matrix. The weighted integral of these unidirectional properties over all directions yields the material stiffness tensor expectation, where the weight function is the fiber orientation distribution. The domain of integration must be sufficiently large enough to contain many fibers yet smaller that the length scale of the global stress and deformation fields. In this way the basic assumption for a continuum model is satisfied. Estimates of the elastic properties for the underlying unidirectional stiffness matrix can be obtained using many desired micromechanics theories, such as that of Halpin-Tsai [27], Mori-Tanaka [28], Tandon-Weng [29] or even the rule of mixtures. However the rule of mixtures is not suggested as it assumes all fibers are infinite in length, thus significantly over predicting the actual stiffness. Based on the work of Tucker and Liang [30], we use the method of Mori-Tanka [28] using the form of Tandon and Weng [29], as they suggest the Mori-Tanaka equations provide reasonable results compared to the idealized solutions from full finite element solutions.

Advani and Tucker [4] hypothesized and Jack and Smith [26] proved that the expectation of the fourth-order material stiffness tensor can be expressed in terms of the orientation tensor as

$$\begin{aligned}\langle C_{ijkl(\mathrm{P})}\rangle = {} & B_1(a_{ijkl}) + B_2(a_{ij}\delta_{kl} + a_{kl}\delta_{ij}) \\ & + B_3(a_{ik}\delta_{jl} + a_{il}\delta_{jk} + a_{jl}\delta_{ik} + a_{jk}\delta_{il}) \\ & + B_4(\delta_{ij}\delta_{kl}) + B_5(\delta_{ik}\delta_{jl} + \delta_{il}\delta_{jk})\end{aligned} \tag{20}$$

where the B_i's are scalars related to the five independent components of the underlying unidirectional stiffness tensor given as

$$\begin{aligned} B_1 &= C_{11} + C_{22} - 2C_{12} - 4C_{66} \\ B_2 &= C_{12} - C_{23} \\ B_3 &= C_{66} + \frac{1}{2}(C_{23} - C_{22}) \\ B_4 &= C_{23} \qquad B_5 = \frac{1}{2}(C_{22} - C_{23}) \end{aligned} \tag{21}$$

COMPUTED RESULTS

The equation of motion of the second order orientation tensor of Equation (5) was solved using 4 different closure approximations: (1) the Hybrid, (2) the orthotropic ORT closure, (3) the Neural Network (NNET), (4) the Orthotropic Neural network (NNORT). The orientation was also solved using the FEC closure to solve the coupled Equations (18) and (19). The orientation information is then used to predict the resulting material properties if the filling of the composite part were to stop at the given instant of time and the part were allowed to cure. All results are compared those obtained from the orientation solution obtained from the Spherical Harmonic approach of Equation (2). This solution (labeled SPH) is considered to be numerically exact, and can be used to validate a particular closure approach.

Two flow conditions are considered to investigate the viability of the exact closure. For both scenarios, the fiber aspect ratio is $r_e = 10$, thus the parameter of orientation for Equation (5) is $\lambda = (10^2-1)/(10^2+1) \approx 0.98$. Predictions of the elastic properties are made based on the Tendon-Weng model [17] in conjunction with Equation (20). The properties of the fiber reinforced thermoplastic considered in the following examples are [19]

$$\begin{aligned} &E_f = 30\times10^9\text{Pa} \qquad v_f = 0.2 \qquad V_f = 0.2 \\ &E_m = 1\times10^9\text{ Pa} \qquad v_m = 0.38 \end{aligned} \tag{22}$$

where V_f is the volume fraction of fibers, E_f is the Young's modulus of the fiber, E_m is the Young's modulus of the matrix, v_f is the fiber Poisson's ratio, and v_m is the matrix Poisson's ratio.

Flow #1 Simple shear

The fluid velocity vector components for simple shear are given as $v_1 = Gx_3$, $v_2 = v_3 = 0$ with an interaction coefficient of $C_I = 10^{-2}$. Simple shear is chosen for two reasons. The primary reason is due to the regularity that shearing flows occur in industrial processes, and thus all closures must be tested in this case. The second reason is due to the propensity of pure shearing flow to show the limitations of a closure due to the periodic nature of the fiber orientation when there are no fiber collisions present.

Results from the solutions of the equation of motion for a_{ij} are provided in Figure 1 from each of the aforementioned closure methods. A look at the second order orientation tensor results shows that the FEC and the ORT yield numerically identical results (out to the third significant digit), with the Hybrid performing the poorest and the neural network closures with the most accurate results. The observation that the neural network closures are the most accurate is not surprising as these observations were provided previously in [5,17]. But the results from the FEC have not been previously observed, and it is intriguing that both the ORT and the FEC are both constructed independent of any flow conditions, whereas the neural networks and other orthotropic closures are constructed based on fitting the closure form to data available from numerical solutions of the full orientation distribution function. Thus it is anticipated that closures based on fiber orientation data may have select orientation states where the solution will yield nonsensical results, and

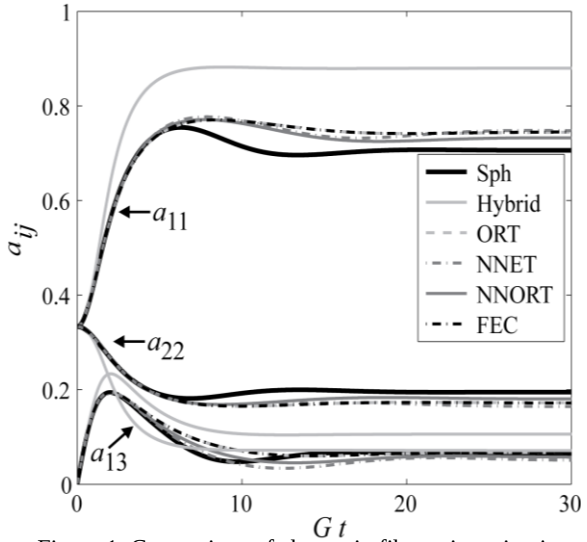

Figure 1: Comparison of change in fiber orientation in simple-shear flow for $\boldsymbol{C_I = 10^{-2}}$ and $\boldsymbol{r_e = 10}$.

has been a problem for many of the fitted closures. The ORT is still obtained from a fitting process, but it is obtained independent from solving the equation of motion of the fiber orientation distribution function, and is thus one of the most robust closures available. It is quite promising that the FEC closure yields results that are identical to the robust ORT, and more promising in that it does not rely on a fitting process thus eliminating the concern with using a function for a region that is significantly different than the fit.

Of importance is the structural response of the processed composite material. As previously mentioned in Equation (20), the structural stiffness can

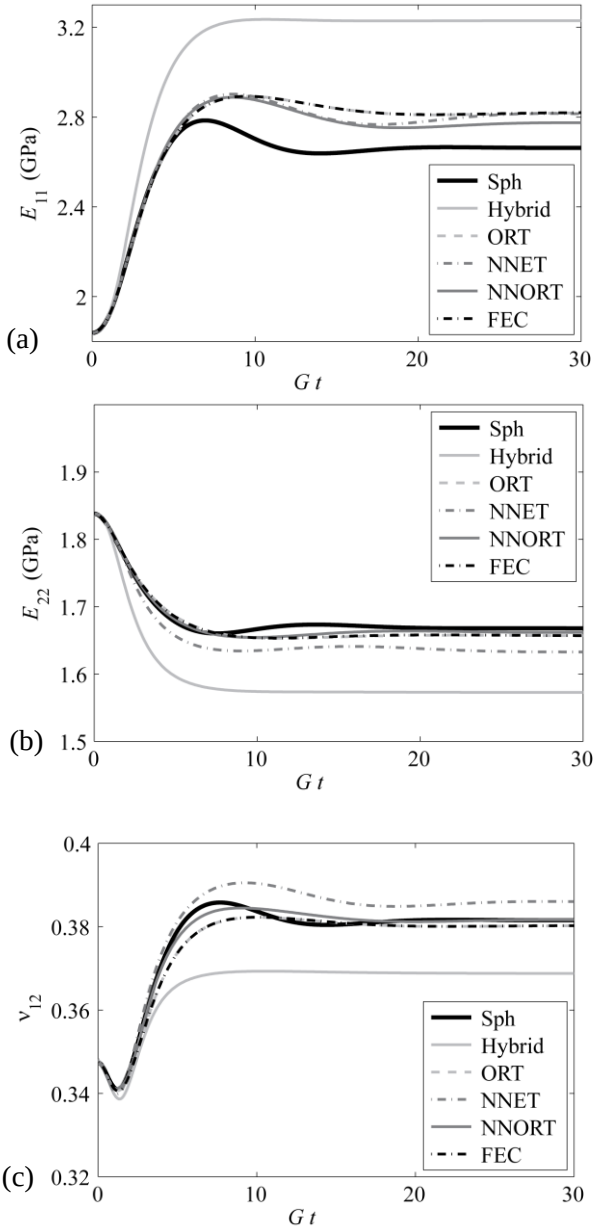

Figure 2: Comparison of (a) longitudinal modulus $\boldsymbol{E_{11}}$ (b) transverse modulus $\boldsymbol{E_{22}}$ and (c) Poisson's Ratio $\boldsymbol{\nu_{12}}$ for a cured part fabricated under a pure shearing flow at select processing times for $\boldsymbol{C_I = 10^{-2}}$ and $\boldsymbol{r_e = 10}$.

be obtained from the second- and fourth-order orientation tensor. Three elastic properties are

presented; E_{11}, E_{22}, and v_{12}, which are, respectively, Young's modulus in the x_1 direction longitudional to the flow direction, Young's modulus in the x_2 direction transverse to the flow direction and the plane of shear, and Poisson's ratio on the x_1 face in the x_2 direction. Each of these property parameters are shown, respectively, in Figure 2. The figure can be interpreted as the material stiffness at a point that at time $t = 0$ had an isotropic orientation state, and that after time Gt the flow was stopped, and the part was allowed to cure. Observe in Figure 2(a) how the trends of the a_{11} components from the orientation plots for each of the approaches are directly mapped the trends of the E_{11} values, in that E_{11} increases with alignment, and the closer the closure is to capturing the component of a_{11}, the more accurate the prediction is for E_{11}. This characteristic is similar for that of the E_{22} modulus in Figure 2(b). Conversely, the Poisson's ratio is not so easily observed from the orientation behavior, and is harder to qualitatively predict which closure will in general be more accurate. Regardless, the NNORT appears to better represent each of the material stiffness parameters for the flow presented.

The average relative error in the predictions made by the five different closures was computed using

$$\mathrm{Err}_{E_{11}} \equiv \frac{1}{t_f - t_0}\int_{t_0}^{t_f}\left|\frac{E_{11}^{Sph}(t) - E_{11}^{Clos}(t)}{E_{11}^{Sph}(t)}\right| dt \times 100\% \qquad (23)$$

where t_0 is the initial time, t_f is the final time, $E_{11}^{Sph}(t)$ is the Young's modulus obtained from the spherical harmonic solution as a given moment in time, and $E_{11}^{Clos}(t)$ is the Young's modulus obtained from a closure. Similar forms are defined for the remaining stiffness constants. The results for the relative error are given in Table 1 for select material stiffness parameters. It is evident from the results that the neural network closures yield the most accurate results, but the FEC has results that are nearly as accurate, whereas the hybrid closure clearly underperforms as compared to the more sophisticated closures.

Table 1: Relative Error in Select Material Stiffness Parameters for Parts Constructed from a Pure Shearing Flow, with $\boldsymbol{C_I = 10^{-2}}$ and $\boldsymbol{r_e = 10}$.

	NNORT	NNET	FEC	ORT	Hyb
$\mathrm{Err}_{E_{11}}$	3.7%	4.3%	4.9%	4.8%	18%
$\mathrm{Err}_{E_{22}}$	0.4%	1.7%	0.6%	0.6%	5.2%
$\mathrm{Err}_{\nu_{12}}$	0.2%	1.1%	0.5%	0.5%	3.1%
$\mathrm{Err}_{G_{23}}$	1.0%	1.2%	1.3%	1.3%	5.6%
$\mathrm{Err}_{\nu_{21}}$	3.8%	4.7%	5.4%	5.4%	22%

Flow #2 Center Gated disk

Center-gated disk flows is indicative of the flow field near a pin gate [12,26], and regularly occurs in industrial processes. In this type of flow, the fiber suspension enters the mold through a pin gate and flows radially outward. This flow is quite non-homogeneous where the velocity vector $\mathbf{v} = (v_r, v_\theta, v_z)$ is a function of the gap height $2b$ between the wall of the mold and the radial distance r from the gate. Both the velocity and the velocity gradient of a center gated disk can be represented by the following

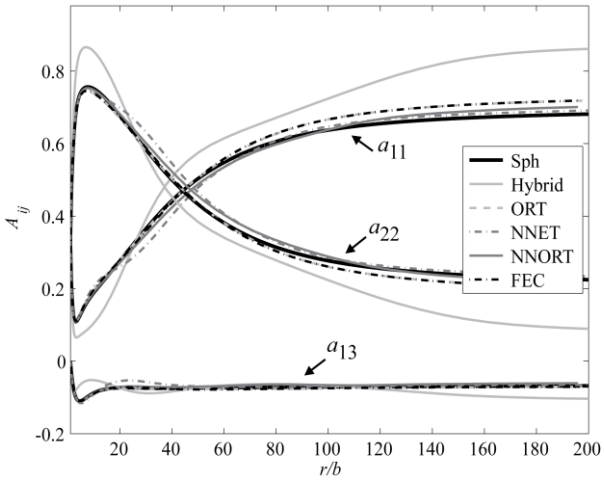

Figure 3: Comparison of change in fiber orientation for center-gated disk flow, $\boldsymbol{z/_b = 2/_{10}}$ $\boldsymbol{C_I = 10^{-2}}$ and $\boldsymbol{r_e = 10}$.

$$v_r = \frac{3Q}{8\pi r b}\left(1 - \left(\frac{z}{b}\right)^2\right) v_\theta = v_z = 0 \qquad (24)$$

$$\frac{\partial v_i}{\partial x_j} = \frac{3Q}{8\pi r b}\begin{bmatrix} -\frac{1}{r}\left(1 - \frac{z^2}{b^2}\right) & 0 & -\frac{2}{b}\frac{z}{b} \\ 0 & \frac{1}{r}\left(1 - \frac{z^2}{b^2}\right) & 0 \\ 0 & 0 & 0 \end{bmatrix} \qquad (25)$$

where z is the gap height location between the mold walls and r denotes the radial location, Q is the volumetric flow rate and b is half the gap thickness. Orientation results are presented in Figure 3 for the gap height $z/_b = 2/_{10}$. Observe how near the gate, the initially isotropic fibers quickly align in the $x_2 = \theta$ direction due to the high elongational flow at the onset, but as they move radially outward from the center of the mold they undergo a high degree of shearing and tend to orient in the $x_1 = r$ direction. As before, the hybrid is the poorest performer, with the neural networks performing with the greatest accuracy, and the ORT and the FEC yielding numerically the same results. This trend is continued when looking at the material stiffness components depicted in Figure 4. It is worthwhile to note that throughout much of the flow history, the ORT and the FEC closures actually better represent the Young's moduli in the tangential direction and Poisson's Ratio than the neural network closures, but it is unclear if this improvement is worth the overestimate of the Young's modulus in the radial direction. Regardless, the NNORT, NNET, ORT and FEC are quite accurate closures, and all yield reasonably accurate results, where the FEC is the only closure that does not rely on a fitting process in its construction.

5. CONCLUSIONS

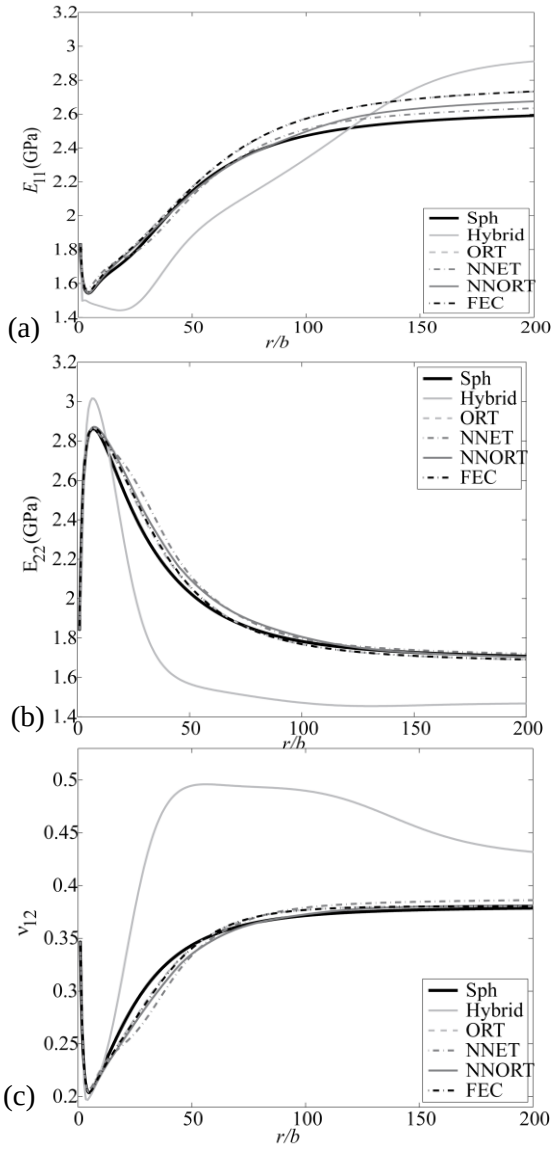

Figure 4: Comparison of (a) longitudional modulus $\boldsymbol{E_{11}}$ (b) transverse modulus $\boldsymbol{E_{22}}$ and (c) Poisson's Ratio $\boldsymbol{\nu_{12}}$ for various radial locations in a cured center-gated disk, $\boldsymbol{z/b = 2/10}$ $\boldsymbol{C_I = 10^{-2}}$ and $\boldsymbol{r_e = 10}$.

We have investigated the orientation tensor and material property prediction of the newly proposed FEC closure and compared those results to those from four other closure approximations. All results are compared to the numerically precise Spherical Harmonic solution of the full orientation distribution function, and all of the recent closures performed quite well. For the orientation prediction and material stiffness predictions, the FEC and the ORT yielded numerically similar results, which is quite promising for the FEC as the ORT is considered by many to be the most accurate and robust closure available to date. Similarly, for the elastic materials properties predicted, the FEC and the ORT closure results were quite reasonable, while the neural network closures, obtained through a sophisticated curve fitting technique, yielded the most accurate results. It can be observed that the results considered show the similarities between the current class of orthotropic fitted closures and that of the novel Fast Exact Closure. Although the results are similar between the fitted closures and the FEC, it is important to recognize that the FEC is formed without a fitting process. Consequently, the results are anticipated, in general, to be more robust in implementation.

ACKNOWLEDGEMENTS

The authors gratefully acknowledge financial support from N.S.F. via grant C.M.M.I. 0727399 as well as Baylor University through their financial support through their new faculty member start-up package.

REFERENCES

[1] Folgar FP, Tucker CL. Orientation Behavior of Fibers in Concentrated Suspensions. *Journal of ReinforcedPlastic Composites*, **3**:98-119, 1984.

[2] Joachim L. The Folgar.Tucker Model as a Differential Algebraic System for Fiber Orientation Calculation, May 2005, Fraunhofer ITWM, Kaiserslautern.

[3] Bay R.S. *Fibre Orientation in Injection Molded Composites: A Comparison of Theory and Experiment*. Ph.D. thesis, University of Illinois at Urbana-Champaign; 1991

[4] Advani S. and C. Tucker. The Use of Tensors to Describe and Predict Fiber Orientation in Short Fiber Composites. *Journal of Rheology*, **31**(8):751-84, 1987.

[5] Jack D.A., B. Schache, and D.E. Smith. Neural Network-Based Closure for Modeling Short-Fiber Suspensions. In Press, *Polymer Composites* 2010.

[6] Jack D.A. and D.E. Smith. The Effect of Fibre Orientation Closure Approximations on Mechanical Property Predictions. *Composites: Part A*, **38**:975-982, 2007.

[7] Advani, S.G. and C.L. Tucker III. Closure Approximations for Three-Dimensional Structure Tensors. *Journal of Rheology*, **34**(3):367-386, 1990.

[8] Doi M. Molecular Dynamics and Rheological Properties of Concentrated Solutions of Rod Like Polymers in Isotropic and Liquid Crystalline Phases. *Journal of Polymer Science, Part B, Polymer Physics*, **19**:229-43, 1981.

[9] Hand G.L. A Theory of Anisotropic Fluids. *Journal of Fluid Mechanics*, **13**(1):33-46, 1962.

[10] Cintra J.S. and C.L. Tucker. Orthotropic Closure Approximations for Flow-Induced Fiber Orientation. *Journal of Rheology*, **39**(6):1095-1122, 1995.

[11] Han K.-H., Y.-T. Im. Numerical Simulation of Three-Dimensional Fiber Orientation in Short-Fiber-Reinforced Injection-Molded Parts. *Journal of Materials Processing Technology*, 124:366-371, 2002.

[12] VerWeyst B.E. C.L. Tucker P.H. Foss, and J.F. O'Gara. Fiber Orientation In 3-D Injection Molded Features: Prediction and Experiments. International Polymer Processing, **1999**(4):409-420, 1999.
[13] Chung D.H., T.H. Kwon. Improved Model of Orthotropic Closure Approximation for Flow-Induced Fiber Orientation. *Polymer Composites*, **22**(5):636-49, 2001.
[14] Dupret F., V. Verleye. Modeling the Flow of Fiber Suspensions in Narrow Gaps. In *Advances in the Flow and Rheology of Non-Newtonian Fluids, Part B.* Elsevier, Amsterdam, Netherlands, p. 1347-1398, 1999.
[15] Pretty C.A., S.M. Parks, Shiwei, and M. Shao. Flow-Induced Alignment of Fibers. In: *Proceedings of the ICCM- 12 Conference*. Paris, France 1999
[16] Chung, D.H and T.H Kwon. Invariant-Based Optimal Fitting Closure Approximation for the Numerical Prediction of Flow-Induced Fiber Orientation. *Journal of Rheology*, **46**(1):169-194, 2002.
[17] Qadir N. and D.A. Jack. Modeling Fiber Orientation in Short Fiber Suspensions Using the Neural Network-Based Orthotropic Closure. *Composites: Part A* **40**:1524-1533, 2009.
[18] Montgomery-Smith S., W. He, D.A. Jack, and D.E. Smith. Exact Tensor Closures for the Three Dimensional Jeffery's Equation. Under review, *Journal of Fluid Mechanics*, 2010.
[19] Montgomery-Smith S., D.A. Jack, and D.E. Smith The Fast Exact Closure for Jeffery's Equation with Diffusion. Under review, *Composites, Part A*, 2010.
[20] Montgomery-Smith, S., D.A. Jack and D.E. Smith. Fast Solutions for the Fiber Orientation of Concentrated Suspensions of Short-Fiber Composites Using the Exact Closure Methods. In *Proceedings of the ASME 2010–IMECE*, Vancouver, British Columbia, November 2010.
[21] Montgomery-Smith S., D.A. Jack and D.E. Smith. A Systematic Approach to Obtaining Numerical Solutions of Jeffery's Type Equations Using Spherical Harmonics. *Composites Part A*, **41**(7):827-835, 2010.
[22] Weisstein, E.W. Spherical Harmonic. Taken from *Mathworld-A Wolfram Web Resource*, http://mathworld.wolfram.com/SphericalHarmonic.html, 2010.
[23] Jeffery, G.B. The Motion of Ellipsoidal Particles Immersed in a Viscous Fluid. *Proceedings of the Royal Society of London A*, **102**:161-179, 1923.
[24] Jack D.A. and D.E. Smith. An Invariant Based Fitted Closure of the Sixth-Order Orientation Tensor for Modeling Short-Fiber Suspensions. *Journal of Rheology*, **49**(5):109-115, 2005.
[25] Dray, D., P. Gilormini and G. Régnier. Comparison of Several Closure Approximations for Evaluating the Thermoelastic Properties of an Injection Molded Short-Fiber Composite. *Composites Science and Technology*, **67**(7-8):1601-1610, 2007.
[26] Jack, D.A. and D.E. Smith, D.E. Elastic Properties of Short-Fiber Polymer Composites, Derivation and Demonstration of Analytical Forms for Expectation and Variance from Orientation Tensors. *Journal of Composite Materials*, **42**(3):277-308, 2008.
[27] Halpin, J. C. and J.L. Kardos, J. L. The Halpin-Tsai Equations: A Review. *Polymer Engineering and Science*, **16**(5):344-352, 1976.
[28] Mori T. and K. Tanaka. Average Stress in Matrix and Average Elastic Energy of Materials with Misfitting Inclusions. *Acta Metallurgica*, **21**:571-574, 1973.
[29] Tandon, G.P. and G.J. Weng. The Effect of Aspect Ratio of Inclusions on the Elastic Properties of Unidirectionally Aligned Composites. *Polymer Composites*, **5**(4):327-333, 1984.
[30] Tucker C.L. and E. Liang. Stiffness Predictions for Unidirectional Short-Fiber Composites: Review and Evaluation. *Composites Science and Technology*, **59**:655–671, 1999.

